QTAIM investigation of a dipyrazol-1-ylmethane derivative and its Zn(II) complexes (ZnLX$_2$, X = Cl, Br or I)

MARYAM DEHESTANI and LEILA ZEIDABADINEJAD*

Department of Chemistry, Shahid Bahonar University of Kerman, 76169 Kerman, Iran

Abstract: Topological analyses of the electron density were performed on the bis(pyrazol-1-yl)methane derivative 9-(4-(di-1*H*-pyrazol-1-ylmethyl)phenyl)- -9*H*-carbazole (**L**) and its zinc(II) complexes: ZnLCl$_2$ (**1**), ZnLBr$_2$ (**2**) and ZnLI$_2$ (**3**) using the quantum theory of atoms in molecules (QTAIM) at the B3PW91/6-31g(d) theoretical level. The topological parameters derived from the Bader theory were also analyzed; these are characteristics of Zn-bond critical points and of ring critical points. The calculated structural parameters were the frontier molecular orbital energies, the highest occupied molecular orbital energy (E_{HOMO}), the lowest unoccupied molecular orbital energy (E_{LUMO}), hardness (η), softness (S), the absolute electronegativity (χ), the electrophilicity index (ω) and the fractions of electrons transferred (ΔN) from ZnLX$_2$ complexes to **L**. Numerous correlations and dependencies between the energy terms of the symmetry adapted perturbation theory approach (SAPT), geometrical, topological and energetic parameters were detected and are described.

Keywords: ZnLX$_2$; charge transfer; bond critical point; SAPT.

INTRODUCTION

The coordination chemistry of di/poly-pyrazolylmethane has seen significant development during the past few years.[1,2] One of the current interesting topics is to rationally design and synthesize supramolecular structures based on di/poly- -pyrazolylmethane units, which are capable of multiple binding modes and have the potential to participate in important non-covalent interactions that direct their self-assembly into remarkable architectures.[3] Compared with coordination bonds, non-covalent forces are weaker, but they are common and play critical roles in the formation of supramolecular structures due to their significant contribution to the self-assembly process.[4–6] More studies focused on the weak non-covalent forces in the design and synthesis of supramolecular structures. Herein, the

---

dipyrazol-1-ylmethane derivative 9-(4-(di-1*H*-pyrazol-1-ylmethyl)phenyl)-9*H*-
-carbazole (L) and its zinc(II) complexes: $ZnLCl_2$ (**1**), $ZnLBr_2$ (**2**) and $ZnLI_2$ (**3**)
are reported. The ligand L, $ZnLBr_2$ and $ZnLI_2$ were synthesized by Wang *et al.*[7]
In the solid state, each compound showed extensive non-covalent interactions,
including weak hydrogen bonds and $C\cdots H\cdots\pi$ interactions that organize the
molecules into 2D and 3D structures. It could be stated that such interactions are
common not only in the present compounds but also in a large number of known
polypyrazolylborate and polypyrazolylmethane compounds.

QTAIM,[8] the chemical bonds in both isolated species and molecular crystals
can be classified and quantified in terms of features of the bond critical points in
the electron density, both theoretically and experimentally. The variety of the
atomic interactions can be approximately divided into shared (or covalent) inter-
actions, intermediate (partially covalent) interactions and closed-shell (van der
Waals, ionic, metal, *etc.*) interactions.[9–11] The fundamental differences between
the two limiting extremes in the interactions, *i.e.*, closed-shell interactions and
shared ones, are the electron density features at the bond critical point. These are
the value of electron density, ρ_b, and the sign of the Laplacian of the electron
density, $\nabla^2\rho_b$, as well as the energy density $H_{e,b} = G_b + V_b$, where V_b and G_b are
the potential and kinetic energy densities, respectively.[10,11] Shared interactions
exhibit $\rho_b \geq 0.14$ au, $\nabla^2\rho_b < 0$ and $H_b < 0$, while closed-shell interactions show
$\rho_b \leq 0.05$ au, $\nabla^2\rho_b > 0$ and $H_b > 0$. In the intermediate region, $\nabla^2\rho_b(r) > 0$ and
$H_b(r) < 0$.

The term non-covalent interaction may be ambiguous since covalency is
attributed not only to typical chemical bonds. It is also connected with the hyd-
rogen bond and with the other interactions, such as halogen or dihydrogen bonds.
Covalency is usually attributed to charge transfer and polarization interaction
energy contributions. It seems that there are meaningful differences between the
interaction mentioned above, such as ionic bond and covalent bonds. The goal of
this study was to apply density functional theory (DFT) calculations[12] and the
QTAIM theory[13] to analyze the properties of the $N\cdots Zn–X$ bonds in $ZnLCl_2$,
$ZnLBr_2$ and $ZnLI_2$. The latter gives direct information on the presence and type
of chemical bonds in these structures.

<div align="center">COMPUTATIONAL DETAILS</div>

All calculations, including optimizations were performed with Gaussian 03 sets of code[13]
using the B3PW91/6-31G(d) level of theory without any symmetry restrains. Quantum chem-
ical calculations of L based on density functional theory was performed at the B3PW91/
/631G(d) level and calculations of complexes **1**–**3** were realized with B3PW91/6–31G(d) for
the C, H, N, Cl, Br and I atoms and the LANL2DZ basis set for the Zn atoms.

QTAIM was also applied, and the characteristics of the bond critical points (BCPs) and
ring critical points (RCPs) were analyzed in terms of the following properties: the electron
density at the critical point, its Laplacian and the total electron energy density at the critical
point. For the latter, its components were also investigated: the potential electron energy

density and the kinetic electron energy density. The following relations are well known if all terms are expressed in atomic units:

$$\frac{1}{4}\nabla^2\rho_b = 2G_b + V_b \tag{1}$$

$$H_{e,b} = G_b + V_b \tag{2}$$

The symmetry adapted perturbation theory (SAPT) approach was applied to deepen the understanding of the nature of the interactions[14] for complexes **1**–**3**. The MOLPRO package[15] was used to perform the calculations. SAPT is a well-established approach to calculate the interaction energy of two closed-shell moieties, whereby the interaction energy is obtained directly as the sum of defined contributions. Thus, it is different from the commonly applied approaches in which the binding energy is calculated as the difference between the energy of the complex and the sum of the energies of the monomers. In the SAPT approach, the interaction energy consists of the following terms: the first-order electrostatics $E_{elst}^{(1)}$, the second-order induction $E_{ind}^{(2)}$ and dispersion $E_{disp}^{(2)}$ energies, and their exchange counterparts: first-order exchange $E_{exch}^{(1)}$, second-order exchange–induction $E_{exch-ind}^{(2)}$ and exchange–dispersion $E_{exch-disp}^{(2)}$. The SAPT method up to the second order gives the main part of the interaction energy. The SAPT2 interaction energy is calculated according to Eq. (3):

$$E_{int}^{SAPT2} = E_{elst}^{(1)} + E_{ind}^{(2)} + E_{disp}^{(2)} + E_{exch}^{(1)} + E_{exch\text{-}ind}^{(2)} + E_{exch\text{-}disp}^{(2)} + \delta E_{HF} \tag{3}$$

RESULTS AND DISCUSSION

Structure of the ligand

Ligand L crystallizes in the monoclinic space group P2$_1$, selected bond distances and angles are listed in Table I. The molecular structure of L and its 1D linear chain are shown in Fig. 1. The dihedral angles between the carbazole ring and the central phenyl unit are 44.3° in molecule **a** and 46.9° in molecule **b**. In molecule **a**, the dihedral angles of the central phenyl unit and the pyrazole rings (R1, R2) are 71.4 and 80.4°, respectively. The dihedral angle of the two pyrazole rings (R1, R2) is 54.9°. In molecule **b,** the dihedral angles of the central phenyl unit and the pyrazole rings (R3, R4) are 71.8 and 80.0°, respectively. The dihedral angle of the two pyrazole rings (R3, R4) is 55.5°. There is no extended conjugation among the carbazole, phenyl and pyrazole rings.

In the molecular structure of complexes **1**-**3**, the Zn(II) ion is four coordinated by two nitrogen atoms of the pyrazolyl groups (L) and two halogen ions to form a distorted tetrahedral geometry. The two pyrazole groups linked to Zn(II) lead to changes in the structure of the ligand. In the structure of ZnLCl$_2$, shown in Fig. 2, the dihedral angles between the carbazole ring and the phenyl unit, between the phenyl unit and the pyrazole rings, and between the two pyrazole rings are 60, 78 and 77, and 52°, respectively. The dihedral angles between the carbazole ring and the phenyl unit, and between the phenyl unit and pyrazole rings are larger than those of the free ligand are. However, the dihedral angle of the two pyrazole rings is smaller than that observed for the free ligand, indicating that

DEHESTANI and ZEIDABADINEJAD

TABLE I. Calculated geometry parameters of L, ZnLCl$_2$, ZnLBr$_2$ and ZnLI$_2$

Cmpd.	Bond length, Å		Bond angle, °	
L	N1–N3	1.3411	N3–N1–C1	120.45
	N2–N4	1.3442	N4–N2–C1	121.36
	N1–C1	1.4546, (1.451)[9]	N1–C1–H1	104.77
	N2–C1	1.4453, (1.455)[9]	N2–C1–H1	106.38
	C1–C2	1.5112, (1.523)[9]	N1–C1–N2	110.65, (110.7)[9]
	C1–H1	1.1064	C2–C1–H1	108.59
Complex **1**	N1–N3	1.3474	N3–N1–C1	110.73
	N2–N4	1.3479	N4–N2–C1	110.73
	N1–C1	1.4544	N1–C1–H1	104.76
	N2–C1	1.4447	N2–C1–H1	106.31
	C1–C2	1.5110	N1–C1–N2	110.73
	C1–H1	1.1019	C2–C1–H1	108.64
	Zn–Cl1	2.2091	N3–Zn–N4	86.97
	Zn–Cl2	2.1960	N3–Zn–Cl1	105.77
	Zn–N3	2.0848	N3–Zn–Cl2	112.71
	Zn–N4	2.0779	N4–Zn–Cl1	104.73
Complex **2**	N1–N3	1.3466	N3–N1–C1	120.95
	N2–N4	1.3478	N4–N2–C1	120.87
	N1–C1	1.4545	N1–C1–H1	104.75
	N2–C1	1.4447	N2–C1–H1	106.31
	C1–C2	1.5109	N1–C1–N2	110.72
	C1–H1	1.1019	C2–C1–H1	108.65
	Zn–Br1	2.3033, (2.364)[9]	N3–Zn–N4	86.76, (89.29)[9]
	Zn–Br2	2.2993, (2.355)[9]	N3–Zn–Br1	106.08, (109.6)[9]
	Zn–N3	2.1019, (2.071)[9]	N3–Zn–Br2	110.89, (120.4)[9]
	Zn–N4	2.1007, (2.064)[9]	N4–Zn–Br1	104.15, (108.0)[9]
Complex **3**	N1–N3	1.3913	N3–N1–C1	120.27
	N2–N4	1.3895	N4–N2–C1	120.54
	N1–C1	1.4545	N1–C1–H1	104.75
	N2–C1	1.4447	N2–C1–H1	106.31
	C1–H1	1.1019	C2–C1–H1	108.65
	Zn–I1	2.5109, (2.550)[9]	N3–Zn–N4	91.57, (88.74)[9]
	Zn–I2	2.4882, (2.533)[9]	N3–Zn–I1	106.39, (108.3)[9]
	Zn–N3	1.9468, (2.057)[9]	N3–Zn–I2	116.78, (115.1)[9]
	Zn–N4	1.9448, (2.050)[9]	N4–Zn–I1	108.28, (109.1)[9]

the planarity of ligand in complex 1 is worse than that for the free ligand. The Zn–N3 and Zn–N5 bond lengths are 2.0848 and 2.0779 Å, respectively. The bond distances of Zn–Cl1 and Zn–Cl2 are 2.2091 and 2.1960 Å, respectively. In complexes **2** and **3**, the changes in the structure of ligand are similar to that of complex **1**. The planarity of coordinated ligand is also worse than that of the free ligand. The corresponding angles and bond lengths for complexes **2** and **3** are listed in Table I and displayed in Figs. 3 and 4.
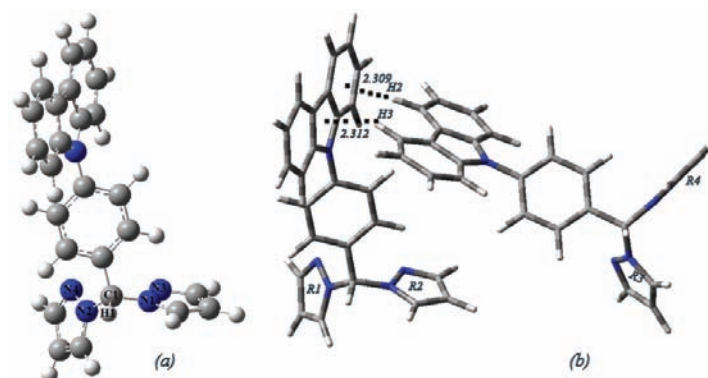
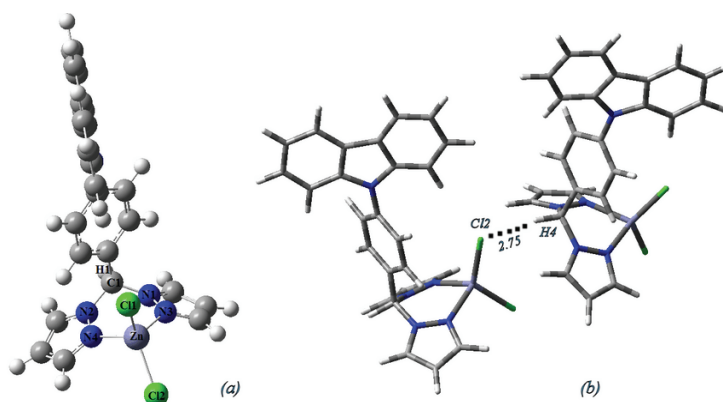Fig. 1. a) The molecular structure of L and b) the 1D linear chain of ligand L. The bond lengths are in Å.

Fig. 2. a) The molecular structure of complex **1** and b) the 1D structure of complex **1** showing the weak C–H···Cl bond in Å.
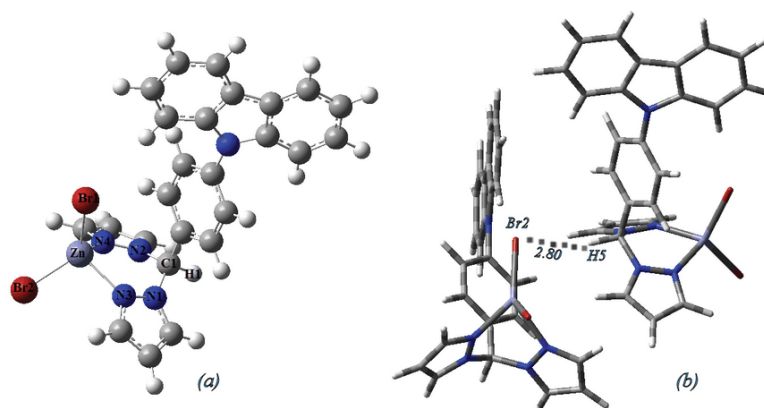

Fig. 3. a) The molecular structure of complex **2** and b) the 1D structure of complex **2** showing the weak C–H···Br bond in Å.
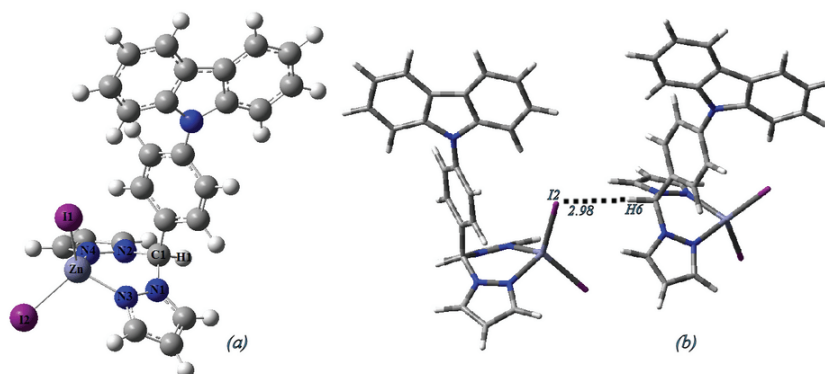
Fig. 4. a) The molecular structure of complex **3** and b) the 1D structure of complex **3** showing the weak C—H···I bond in Å.

Global reactivity descriptors

A large part of theoretical chemistry related to reactivity is based on the concept of frontier molecular orbitals (FMO), especially the lowest unoccupied molecular orbital (LUMO) and the highest occupied molecular orbital (HOMO). The interaction between these orbitals often allows a good description of the reactivity of reactions. The FMO theory says that the attack of an electrophilic species will occur where there is more density of the HOMO, whereas the attack of a nucleophilic species will occur in a region with a higher density of the LUMO. Parr and coworkers demonstrated that nearly all the frontier molecular theory could be rationalized from the DFT.[16]

The μ and molecular η for an N-electron system with total energy E_t and external potential $V(r)$ are defined respectively, as the first and second derivatives of the energy with respect to N:[17,18]

$$\mu = \left[\frac{\partial E}{\partial N}\right]_{V(\vec{r})} = -\chi \tag{4}$$

and

$$\eta = \frac{1}{2}\left[\frac{\partial^2 E}{\partial N^2}\right]_{V(\vec{r})} = \frac{1}{2}\left[\frac{\partial \mu}{\partial N}\right] \tag{5}$$

where χ (eV) in Eq. (4) is the electronegativity. In numerical applications, μ and η are calculated using of the difference approximation:

$$\mu = -\frac{1}{2}\left(IP + E_A\right) \tag{6}$$

$$\eta = \frac{1}{2}\left(IP - E_A\right) \tag{7}$$

The vertical ionization potential (*IP*) and the electron affinity (*E*$_A$) can be obtained from the energy of the neutral, anionic, and the cationic species at the geometry of the corresponding *N* electron neutral species, as follows:

$$IP = \left[E\left(N-1 \right) - E\left(N \right) \right] \tag{8}$$

$$E_A = \left[E\left(N \right) - E\left(N+1 \right) \right] \tag{9}$$

Equations (6) and (7) can be simplified using the Koopmans theorem,[12] which approximates the electronic affinity and the ionization potential to the negative of the LUMO and HOMO energy, respectively.

$$\mu = -\frac{1}{2}\left(E_{LUMO} + E_{HOMO} \right) \tag{10}$$

$$\eta = \frac{1}{2}\left(E_{LUMO} - E_{HOMO} \right) \tag{11}$$

The electrophilicity index (*ω*) and global softness (*S*) are defined as follows:

$$\omega = \frac{\mu^2}{2\eta} \tag{12}$$

$$S = 1/\eta \tag{13}$$

According to Parr *et al.*,[18] *ω* is a global reactivity index similar to the chemical hardness and chemical potential. This new reactivity index measures the stabilization in energy when the system reserves additional electronic charge (*ΔN*). The direction of the charge transfer is determined by the electronic chemical potential of the molecule because an electrophile is a chemical species capable of accepting electrons from the environment; its energy must decrease upon accepting an electronic charge. Thus, its electronic chemical potential must be negative.

The calculated values of *E*$_{HOMO}$, *E*$_{LUMO}$, *χ*, *μ*, *η*, *S* and *ω* for L and its complexes are listed in Table II.

In a reaction between two molecules, species can act as a nucleophile, which has a lower value of the electrophilicity index. The values of the electrophilicity index show that ZnCl$_2$, ZnBr$_2$ and ZnI$_2$ are good nucleophiles; hence, these nucleophiles can attack the ligand L. Electrophilic charge transfer (*ECT*)[19] is explained as the difference between the *ΔN*$_{max}$ values of the interacting molecules. Considering two molecules A (**L**) and B (ZnCl$_2$, ZnBr$_2$ and ZnI$_2$) approaching each other, two cases exist, *i*) *ECT* > 0, charge flow from B to A, *ii*) *ECT* < 0, charge flow from A to B. The *ECT* is calculated as follows:

$$ECT = \left(\Delta N_{max} \right)_A - \left(\Delta N_{max} \right)_B \tag{14}$$

where $(\Delta N_{max})_A = \mu_A / \eta_A$ and $(\Delta N_{max})_B = \mu_B / \eta_B$.

TABLE II. Calculated E_{HOMU}, E_{LUMO}, χ, μ, η, S and ω (in eV) for L, $ZnCl_2$, $ZnBr_2$ and ZnI_2

Molecule	E_{HOMO} / eV	E_{LUMO} / eV	χ / eV	μ / eV	η / eV	S / eV	ω / eV
L	–0.1999	–0.0271	0.1135	–0.1135	0.0864	0.0432	0.0746
$ZnCl_2$	–0.3093	–0.1360	0.2226	–0.2226	0.0867	0.0433	0.2858
$ZnBr_2$	–0.2877	–0.1224	0.2051	–0.2051	0.0826	0.0413	0.2546
ZnI_2	–0.2699	–0.0678	0.1678	–0.1678	0.1010	0.0505	0.1394

The *ECT* was calculated as 1.253, 1.169 and 0.347 for complexes **1**–**3**, respectively. These results show that electrons are transferred from ZnX_2 to L. Therefore, the L was treated as an electron acceptor and, hence, ZnX_2 was treated as an electron donor. Thus, L has electrophilic behavior because the value of chemical potential is low. As shown in Table II, the high value of chemical potential and low value of electrophilicity index for these complexes **1**–**3** favor their nucleophilic behavior.

Local reactivity descriptors

The Fukui function (*FF*)[16,20] or frontier function (f_k^+, f_k^-) measures changes in electron number (removing electrons from the HOMO or adding electrons to LUMO, respectively) in chemical reactions and has been used to predict the reactivity of sites in a molecule. This function is a local density functional descriptor that is calculated using the proposed procedure based on a finite difference method.[21]

In this work, the two functions f^+ and f^- were used to determine electrophilic and nucleophilic attack, respectively. These functions can be given by:

$$f_k^+ = q_k^{(N+1)} - q_k^{(N)} \quad \text{for molecule } k \text{ as an electrophile}$$

$$f_k^- = q_k^{(N)} - q_k^{(N-1)} \quad \text{for molecule } k \text{ as a nucleophile}$$

where the parameters $q_k^{(N)}$, $q_k^{(N-1)}$ and $q_k^{(N+1)}$ are the charges of molecule k calculated in the systems N, N–1 and N+1 electrons, respectively, at the optimized geometry of the molecule with N electrons. In the past few years, the condensed Fukui functions have been used to explain the regioselectivity in chemical reactions.[22] It is a tool that allows the prediction of which electron or moiety of a molecule will display more or less nucleophilic or electrophilic character. Electrophilic reactivity descriptors f_k^+ and nucleophilic reactivity descriptors f_k^- for all molecules are listed in Table III. The maximum values of the nucleophilic reactivity descriptors at Zn indicate that these sites are more prone to electro-

TABLE III. Selected reactivity descriptors indexes of $ZnCl_2$, $ZnBr_2$ and ZnI_2

Molecule	Atom	$q(N)$	$q(N–1)$	$q(N+1)$	f_k^+	f_k^-
$ZnCl_2$	Zn	1.1269	1.2494	0.4060	–0.7208	–0.1226
$ZnBr_2$	Zn	0.9693	1.0814	0.2835	–0.6858	–0.1121
ZnI_2	Zn	0.7296	0.7651	0.0554	–0.6742	–0.0356

philic attack in the $ZnCl_2$ molecule. Thus, it can be stated that the Zn atom attacked the *N* atom of L corresponding in all complexes.

Relationship between geometrical and topological parameters

The calculations performed on the wide spectrum of related species enabled a deeper insight into the characteristics of intramolecular interactions to be obtained. Here, mainly relationships between the bond length and the characteristics of the corresponding bond critical point are considered. For the systems analyzed herein, a pseudo-ring containing the N3···Zn···N4 intramolecular bond is created and hence, an RCP also exist in complexes **1**–**3**. The geometrical and topological parameters of these interactions are presented in Table IV. Briefly summarizing, the greater is the electron density at the RCP of an intramolecular bond, the stronger is the interaction and the shorter is the bond. The Zn···N bond lengths are 2.2091, 2.3033 and 2.5109 Å for complexes **1**–**3**, respectively. The values of $\nabla^2\rho_b$ for complexes **1**–**3** are –0.0201, –0.0388 and –0.0579 au, respectively. As can be seen, the bond length is shorter and the value of $\nabla^2\rho_b$ higher in $ZnLCl_2$ than in the other complexes. Relatively, the values of the $\nabla^2\rho_b$, and

TABLE IV. Topological properties (in au) of the charge density at the bond critical point of L, $ZnLCl_2$, $ZnLBr_2$, and $ZnLI_2$, $\rho(r)$, $\nabla^2\rho(r)$, and G_b, V_b, $H_{e,b}$ and $|V_b|/G_b$

Molecule	Bond	ρ_b	$\nabla^2\rho(r)$	G_b	V_b	$H_{e,b}$	$|V_b|/G_b$
L	N1–C1	0.2772	0.2120	0.1352	0.3472	–0.2120	2.568
	N2–C1	0.2713	0.2030	0.1334	–0.4700	–0.3366	3.523
	C1–H1	0.2744	0.2350	0.0331	–0.3011	–0.2680	9.0967
	N1–N3	0.3748	0.1782	0.2132	–0.6046	–0.3914	2.8358
$ZnLCl_2$	N1–C1	0.2741	0.2070	0.1514	–0.5097	–0.3583	3.3666
	N2–C1	0.2688	0.1998	0.1413	–0.4823	–0.3410	3.4133
	N1–N3	0.3703	0.1768	0.2027	–0.5822	–0.3795	2.8722
	Zn–Cl1	0.0793	–0.0201	0.0829	–0.1157	–0.0328	1.395
	Zn–Cl2	0.0810	–0.0207	0.0849	–0.1192	–0.0343	1.4040
	Zn–N3	0.0722	–0.0620	0.0878	–0.1135	–0.0257	1.2927
	Zn–N4	0.0712	–0.0617	0.0866	–0.1114	–0.0248	1.2863
$ZnLBr_2$	N1–C1	0.2688	0.1998	0.1413	–0.4825	–0.3412	3.4147
	N2–C1	0.2741	0.2073	0.3580	–0.5088	–0.1508	1.4212
	N1–N3	0.3711	0.1775	0.2033	–0.5842	–0.3809	2.8735
	Zn–Br1	0.0782	–0.0388	0.0722	–0.1056	–0.3340	1.4620
	Zn–Br2	0.0779	–0.0393	0.0725	–0.1056	–0.3310	1.4566
	Zn–N3	0.0684	–0.0596	0.0822	–0.1047	–0.0225	1.2737
	Zn–N4	0.0683	–0.0593	0.0818	–0.1043	–0.0225	1.2751
$ZnLI_2$	N1–C1	0.2379	0.0848	0.1232	–0.3313	–0.2081	2.6891
	N2–C1	0.2427	0.0888	0.1276	–0.3441	–0.2165	2.6967
	N1–N3	0.2994	0.1065	0.1660	–0.4385	–0.2725	2.6416
	Zn–I1	0.0559	–0.0579	0.0587	–0.0596	–0.0009	1.0153
	Zn–I2	0.0538	–0.0563	0.0564	–0.0565	–0.0001	1.0018
	Zn–N3	0.0878	–0.1533	0.1571	–0.1608	–0.0037	1.0236
	Zn–N4	0.0882	–0.1538	0.1578	–0.1616	–0.0038	1.0241

$H_{e,b}$, also the values of $1 < |V_b|/G_b < 2$ indicate that the Zn–X (X = Cl, Br and I) and the Zn–N interactions in all complexes have a significant partially covalent component. For the N1–C1, N2–C1, C1–H1 and N1–N3 interactions, the values of the Laplacian are positive, which may mean that the ionic bond could not be classified as very strong one because all $H_{e,b}$ values are negative, which may indicate that such interactions are rather strong. With reducing electronegativity of the X atom connected to Zn(II), the bond strength decreases.

The SAPT calculations

The SAPT applied here seems to be a proper approach to analyze the closed-shell interactions. It was mentioned previously that the nucleophilic attack of Zn atom of ZnX_2 (X = Cl, Br and I) molecules on the ligand L leads to the formation of complexes **1–3**. The SAPT2 interaction energy as well as the interaction energy terms in Eq. (3) are given in Table V. If the attractive (negative) terms of the interaction energy are considered, the induction one, $E_{ind}^{(2)}$, seems to be the most important, followed by the electrostatic term, $E_{elst}^{(1)}$, and the dispersive term. However, the induction and dispersive terms are strongly damped by their exchange counterparts, $E_{exch-ind}^{(2)}$ and $E_{exch-disp}^{(2)}$, respectively. In the case of the induction interaction energy, it is reduced by 70–82 % while for the dispersive energy, its reduction is of 29–30 %. On the other hand, the first order electrostatic energy is outweighed by the first order exchange energy. This shows the role of the induction energy in spite of the fact that the latter one is strongly reduced by its counterpart. There are other observations; the absolute value of the dispersive energy is greater for the complex $ZnLCl_2$ than for the complexes $ZnLBr_2$ and $ZnLI_2$, even if the exchange counterpart of the dispersion energy is taken into account. However all interaction energy terms are interrelated and thus for stronger interaction and consequently shorter intermolecular distance, the absolute values of all interaction energy terms increase.

TABLE V. SAPT interaction energies for the $ZnLI_2$, $ZnLBr_2$ and $ZnLCl_2$ complexes

Energy term, au	$ZnLI_2$	$ZnLBr_2$	$ZnLCl_2$
$E_{elst}^{(1)}$	–9595.54	–10084.66	–10205.6
$E_{ind}^{(2)}$	11217.12	11786.44	11927.80
$E_{disp}^{(2)}$	–18535.24	–19475.99	–19709.57
$E_{exch}^{(1)}$	–3216.07	–3403.57	–3444.39
$E_{exch-ind}^{(2)}$	14696.23	15442.13	15627.33
$E_{exch-disp}^{(2)}$	959.7	1008.46	1020.56
δE_{HF}	–1524.66	–1575.72	–1594.07
E_{int}^{SAPT2}	–5998.46	–6302.91	–6378.50

CONCLUSIONS

The complexes of ligand L and the different non-covalent interactions were considered herein. It was found that for all interactions in which the Zn atom acts as a nucleophile, a relationship between the Zn···N distance and the Laplacian of electron density at the corresponding bond critical point exists. This indicates a region of partially covalent bonds where the Laplacian is negative and the electron density is lower of 0.15 au. Electrophilic charge transfer confirms that the electrons are transferred from the ZnX_2 to the ligand L; thus, the corresponding ligand can be treated as an electron acceptor. The results of Fukui functions indicate Zn atom attack on the N atom of the ligand. The SAPT approach was also applied to analyze interactions in the zinc complexes. It was found that the induction energy is the most important attractive interaction energy term for the studied complexes, followed by electrostatic and dispersive terms. This means that for such strong interactions, the electron density shift is very important for the process of complexation but also that electrostatic interactions steer the arrangement of sub-units in the complexes.

ИЗВОД

 QTAIM ИСПИТИВАЊЕ ДЕРИВАТА ДИПИРАЗОЛ-1-ИЛМЕТАНА И ОДГОВАРАЈУЋИХ Zn(II) КОМПЛЕКСА ($ZnLX_2$, X = Cl, Br ИЛИ I)

MARYAM DEHESTANI[1] и LEILA ZEIDABADINEJAD[1]

Department of Chemistry, Shahid Bahonar University of Kerman, 76169 Kerman, Iran

Применом квантне теорије атома у молекулима (QTAIM) на B3PW91/6-31g(d) нивоу теорије урађена је тополошка анализа електронске густине 9-(4-(ди-1H-пиразол--1-илметил)фенил)-9*H*-карбазола (L) и одговарајућих цинк(II) комплекса: $ZnLCl_2$ (**1**), $ZnLBr_2$ (**2**) и $ZnLI_2$ (3). Анализирани су тополошки параметри добијени применом Бадерове теорије који су карактеристични за критичне тачке координованог цинка и ароматичног прстена. Израчунати су следећи структурни параметри: енергија највише попуњене молекулске орбитале (E_{HOMO}), енергија најниже непопуњене молекулске орбитале (E_{LUMO}), тврди (η) и меки (S) карактер, апсолутна електронегативност (χ), индекс електрофилности (ω) и расподела електрона у комплексу $ZnLX_2$ (ΔN). Описане су корелације између енергије добијене применом SAPT теорије (симетријски прилагођена пертурбациона теорија), геометријских, тополошких и енергетских параметара.

(Примљено 24. фебруара, ревидирано 27. марта, прихваћено 31. марта 2015)

REFERENCES

1. S. Trofimenko, *Chem. Rev.* **93** (1993) 943
2. J. Xia, Z.-J. Zhang, W. Shi, J.-F. Wei, P. Cheng, *Cryst. Growth Des.* **10** (2010) 2323
3. D. L. Reger, R. P. Watson, M. D. Smith, P. J. Pellechia, *Organometallics* **1544** (2005) 24
4. F. Jin, F.-X. Zhou, X.-F. Yang, L.-H. Cheng, Y.-Y. Duan, H.-P. Zhou, L. Kong, F.-Y. Hao, J.-Y. Wu, Y.-P. Tian, *Polyhedron* **43** (2012) 1
5. C. B. Aakeröy, M. Fasulo, N. Schultheiss, J. Desper, C. Moore, *J. Am. Chem. Soc.* **129** (2007) 13772

6. M. Tuikka, M. Niskanen, P. Hirva, K. Rissanen, A. Valkonen, M. Haukka, *Chem. Commun.* **47** (2011) 3427
7. S.-C. Wang, Y.-C. Zhang, F. Jin, W.-D. Liu, H.-P. Zhou, J.-Y. Wu, Y.-P. Tian, *Synth. React. Inorg., Met.-Org. Nano-Met. Chem.* **45** (2015) 639
8. R.F. Bader, *Atoms in molecules,* Wiley Online Library, 1990
9. A. Ranganathan, G. Kulkarni, C. Rao, *J. Phys. Chem., A* **107** (2003) 6073
10. T.-H. Tang, E. Deretey, S. Knak Jensen, I. G. Csizmadia, *Eur. Phys. J., D* **37** (2006) 217
11. P. M. Dominiak, E. Grech, G. Barr, S. Teat, P. Mallinson, K. Woźniak, *Chem. Eur. J.* **9** (2003) 963
12. R. G. Parr, W. Yang, *Density-functional theory of atoms and molecules*, Oxford University Press, New York, 1989, p. 220
13. Gaussian 09, Revision D.01, Gaussian, Inc., Wallingford, CT, 2008
14. B. Jeziorski, R. Moszynski, K. Szalewicz, *Chem. Rev.* **94** (1994) 1887
15. H. J. Werner, P. Knowles, *MOLPRO*, University of Birmingham, 2012
16. R. G. Parr, W. Yang, *J. Am. Chem. Soc.* **106** (1984) 4049
17. P. Geerlings, F. De Proft, W. Langenaeker, *Chem. Rev.* **103** (2003) 1793
18. R. G. Parr, L. V. Szentpaly, S. Liu, *J. Am. Chem. Soc.* **121** (1999) 1922
19. J. Padmanabhan, R. Parthasarathi, V. Subramanian, P. Chattaraj, *J. Phys. Chem., A* **111** (2007) 1358
20. K. Senthilkumar, M. Ramaswamy, P. Kolandaivel, *J. Quantum Chem.* **81** (2001) 4
21. W. Yang, W. J. Mortier, *J. Am. Chem. Soc.* **108** (1986) 5708
22. G. F. Lehr, R. G. Lawler, *J. Am. Chem. Soc.* **106** (1984) 4048.